

Quantum Simulation of Non-Hermitian Linear Response

Jeongbin Jo*

Department of Physics, Yonsei University, Seoul 03722, Republic of Korea

(Dated: March 19, 2026)

Linear response theory and Green's functions provide a universal framework for understanding how macroscopic and strongly correlated systems respond to weak external perturbations. While the theoretical foundation for non-Hermitian linear response theory has been recently established to describe open quantum systems, generalizing these predictions onto practical quantum computers remains a formidable algorithmic challenge due to the non-unitary nature of the dynamics. In this work, we present a systematic algorithmic mapping that transforms the non-unitary multi-time correlation functions into a unitary form viable for quantum hardware. By mapping the vectorization of the Lindblad master equation into a unitary Schrödinger-like equation using the continuous-variable Schrödingerization technique, we show that generalized non-Hermitian Green's functions can be systematically extracted. This approach bridges the gap between the established physical theory of non-Hermitian linear response and quantum simulation, achieving optimal state preparation cost.

I. INTRODUCTION

The linear response theory has given a general proof of the fluctuation-dissipation theorem, which states that the linear response of a given system to an external perturbation is expressed in terms of fluctuation properties of the system in thermal equilibrium. Such a response is characterized by a response function or admittance, and the internal fluctuation is characterized by a correlation function [1, 2].

In the study of strongly correlated electron systems, such as the Fermi-Hubbard model, evaluating single-particle correlation functions and Green's functions is a primary objective. Recent quantum algorithms have successfully accessed these Green's functions directly by using an analog of the Kubo formula. However, these direct measurements are strictly restricted to closed systems evolving under a Hermitian Hamiltonian $H(t) = H^\dagger(t)$. Dealing with non-unitary processes, such as dissipation or continuous measurements, presents a fundamental barrier.

Recently, the theoretical framework of linear response has been elegantly extended to non-Hermitian regimes by Pan et al. [3], providing a robust physical foundation for understanding dynamical responses to dissipative probes. However, translating this non-Hermitian response theory into a viable quantum simulation algorithm reveals a critical bottleneck: the time evolution operator $e^{\mathcal{L}t}$ is fundamentally non-unitary. Traditional approaches to simulating such non-unitary dynamics often rely on dilated linear system solvers or the spectral mapping theorem, which incur exponential overheads in circuit depth and state preparation.

In this paper, we bridge the fundamental gap between the physical formalism of non-Hermitian response theory [3] and quantum computational implementation. We propose a novel quantum algorithmic protocol that utilizes the Schrödingerization technique [4] to compute non-equilibrium Green's functions and two-time correlation

functions $\langle A(t)B(0) \rangle$. By elevating the non-unitary dynamics into an extended unitary evolution, our framework provides the first scalable algorithmic pathway to simulate dissipative responses without the exponential overhead of traditional dilated system solvers.

II. THEORETICAL FRAMEWORK

A. Vectorization and the Quantum Regression Theorem

Consider an open quantum system whose density matrix $\rho(t)$ evolves according to the Lindblad master equation. By vectorizing the density matrix into a state $|\rho(t)\rangle$ in the Liouville space, the dynamics is governed by a non-Hermitian superoperator \mathcal{L} :

$$\frac{d}{dt} |\rho(t)\rangle = \mathcal{L} |\rho(t)\rangle. \quad (1)$$

According to the Quantum Regression Theorem, the two-point correlation function for observables A and B can be evaluated as:

$$\langle A(t)B(0) \rangle = \langle I | (A \otimes I) e^{\mathcal{L}t} (B \otimes I) | \rho(0) \rangle. \quad (2)$$

Calculating this dynamically requires simulating the non-unitary propagator $e^{\mathcal{L}t}$, which is not directly executable as a quantum gate. The explicit mapping to the Liouville space via vectorization [5, 6] is detailed in Appendix A.

B. Schrödingerization of the Lindbladian

To simulate the non-unitary term $e^{\mathcal{L}t}$, we employ the Schrödingerization method. We first decompose the generator $\mathcal{L} = \mathcal{H}_1 - i\mathcal{H}_2$, where both \mathcal{H}_1 and \mathcal{H}_2 are Hermitian. We introduce a real one-dimensional variable $\xi > 0$ and apply the warped phase transformation [4]:

$$w(t, \xi) = e^{-\xi} |\rho(t)\rangle. \quad (3)$$

* jeongbin033@yonsei.ac.kr

Let $\tilde{w}(t, \eta)$ be the Fourier transform of w in ξ , and $\eta \in \mathbb{R}$ be the Fourier mode. Then \tilde{w} satisfies a system of uncoupled Schrödinger-like equations:

$$i\partial_t \tilde{w} = (\eta \mathcal{H}_1 + \mathcal{H}_2) \tilde{w}. \quad (4)$$

This Hamiltonian $\mathcal{H}_{sch}(\eta) = \eta \mathcal{H}_1 + \mathcal{H}_2$ is now Hermitian, allowing unitary evolution on a quantum computer. A step-by-step derivation of the phase transformation and the Fourier mapping [7] is provided in Appendix B.

C. Non-Hermitian Linear Response and Green's Functions

Beyond simple correlation functions, the response of a strongly correlated system to a weak external perturbation is formally captured by Green's functions. Suppose the Lindbladian is perturbed as $\mathcal{L} \rightarrow \mathcal{L} + \delta\mathcal{L}(t)$, where $\delta\mathcal{L}(t) = f(t)\mathcal{V}$. The linear change in the expectation value of an observable A is given by:

$$\delta\langle A(t) \rangle = \int_0^t \chi(t-t') f(t') dt', \quad (5)$$

where the non-Hermitian response function $\chi(\tau)$ acts as the generalized retarded Green's function for the open system:

$$\chi(\tau) = \langle I | (A \otimes I) e^{\mathcal{L}\tau} \mathcal{V} | \rho_{eq} \rangle. \quad (6)$$

In closed systems, this response is evaluated using the Kubo formula. By treating $\mathcal{V} | \rho_{eq} \rangle$ as the initial vectorized state, the term $e^{\mathcal{L}\tau} \mathcal{V} | \rho_{eq} \rangle$ can be simulated via Schrödingerization. This conceptual mapping formally extends the Kubo formula evaluation of Green's functions to dissipative, non-Hermitian regimes on quantum hardware. The rigorous derivation of the response function for non-unitary generators [3] is shown in Appendix C.

D. Complexity and Scaling

Compared to block-encoding techniques like Generalized Quantum Signal Processing (GQSP) [8], the Schrödingerization approach scales as $O(\text{poly}(\log(1/\epsilon)))$ in terms of precision ϵ . Furthermore, following the LCHS paradigm [9, 10], our method avoids the unfavorable state preparation costs associated with non-unitary matrix inversion algorithms (like HHL [11] or QSVT [12] for non-unitary operators), making it a near-optimal candidate for high-dimensional open system simulations. A detailed comparison of various quantum simulation primitives is provided in Table I, and the formal error-bound derivation is presented in Appendix E.

III. APPLICATION: SINGLE-QUBIT AMPLITUDE DAMPING

To analytically validate our framework without relying on numerical heuristics, we explicitly derive the Schrödingerization mapping for a fundamental open quantum system: a single qubit undergoing spontaneous emission (the amplitude damping channel).

Let the system Hamiltonian be $H_S = \frac{\omega_0}{2} \sigma_z$. The interaction with the vacuum environment is described by the Lindblad master equation with a decay rate γ :

$$\frac{d\rho}{dt} = -i[H_S, \rho] + \gamma \left(\sigma_- \rho \sigma_+ - \frac{1}{2} \{ \sigma_+ \sigma_-, \rho \} \right), \quad (7)$$

where $\sigma_- = |0\rangle\langle 1|$ and $\sigma_+ = |1\rangle\langle 0|$ are the lowering and raising operators, respectively.

We vectorize the density matrix ρ into a column vector $|\rho\rangle = (\rho_{11}, \rho_{10}, \rho_{01}, \rho_{00})^T$ in the Liouville space. The master equation is recast into a system of linear ODEs governed by a 4×4 non-Hermitian matrix \mathcal{L} :

$$\mathcal{L} = \begin{pmatrix} -\gamma & 0 & 0 & 0 \\ 0 & -i\omega_0 - \frac{\gamma}{2} & 0 & 0 \\ 0 & 0 & i\omega_0 - \frac{\gamma}{2} & 0 \\ \gamma & 0 & 0 & 0 \end{pmatrix}. \quad (8)$$

Following the Schrödingerization protocol, we decompose \mathcal{L} into its Hermitian (\mathcal{H}_1) and anti-Hermitian (\mathcal{H}_2) components: $\mathcal{L} = \mathcal{H}_1 - i\mathcal{H}_2$, defined as $\mathcal{H}_1 = (\mathcal{L} + \mathcal{L}^\dagger)/2$ and $\mathcal{H}_2 = i(\mathcal{L} - \mathcal{L}^\dagger)/2$. A straightforward algebraic manipulation yields:

$$\mathcal{H}_1 = \begin{pmatrix} -\gamma & 0 & 0 & \frac{\gamma}{2} \\ 0 & -\frac{\gamma}{2} & 0 & 0 \\ 0 & 0 & -\frac{\gamma}{2} & 0 \\ \frac{\gamma}{2} & 0 & 0 & 0 \end{pmatrix}, \quad (9)$$

and

$$\mathcal{H}_2 = \begin{pmatrix} 0 & 0 & 0 & -i\frac{\gamma}{2} \\ 0 & \omega_0 & 0 & 0 \\ 0 & 0 & -\omega_0 & 0 \\ i\frac{\gamma}{2} & 0 & 0 & 0 \end{pmatrix}. \quad (10)$$

By transforming to the Fourier space η , the extended Hamiltonian governing the unitary evolution of the continuous-variable state $\tilde{w}(t, \eta)$ becomes $\mathcal{H}_{sch}(\eta) = \eta \mathcal{H}_1 + \mathcal{H}_2$:

$$\mathcal{H}_{sch}(\eta) = \begin{pmatrix} -\eta\gamma & 0 & 0 & \frac{\gamma}{2}(\eta - i) \\ 0 & -\frac{\eta\gamma}{2} + \omega_0 & 0 & 0 \\ 0 & 0 & -\frac{\eta\gamma}{2} - \omega_0 & 0 \\ \frac{\gamma}{2}(\eta + i) & 0 & 0 & 0 \end{pmatrix}. \quad (11)$$

Crucially, $\mathcal{H}_{sch}(\eta)$ is perfectly Hermitian for any real η . This rigorous mapping proves that the non-unitary Lindblad dynamics associated with correlation functions can

TABLE I. Comparison of Quantum Simulation Primitives for Non-Unitary Dynamics. Here, ϵ denotes target precision.

Method	Precision Scaling	State Preparation	Oracle Requirement
Dilation [11]	$O(\text{poly}(1/\epsilon))$	High (Block-encoding)	U_A, P_b
QSVT / GQSP [8, 12]	$O(\log(1/\epsilon))$	High (Block-encoding)	U_A , Ancilla
LCHS [9]	$O(\text{poly}(\log(1/\epsilon)))$	Optimal	Hamiltonian
Schrödingerization [4]	$O(\text{poly}(\log(1/\epsilon)))$	Optimal	Unitary Propagator

be structurally elevated to a unitary Schrödinger equation. To calculate the response to an external drive, such as $H_{ext} = \epsilon \cos(\Omega t) \sigma_x$, one simply sets the initial state of the Schrödingerized evolution to $|\mathcal{V}\rho_{eq}\rangle$, where \mathcal{V} is the Liouvillian perturbation representing the σ_x drive. The resulting time evolution on the quantum computer then yields the generalized Green's function $\chi(\tau)$, confirming the validity of the Non-Hermitian Response Theory on quantum hardware.

IV. NUMERICAL DEMONSTRATION

To validate the theoretical framework and the precision of the Schrödingerization mapping, we performed quantum circuit simulations on a single-qubit amplitude damping model described in Section III. The non-unitary correlation function requires generating the unitary operator $e^{-i\mathcal{H}_{sch}(\eta)t}$ and taking the expectation value with respect to the initial state. To extract the real part of this overlap in a quantum hardware-compatible manner, we employ the Hadamard test. For our 2-qubit vectorized Liouville system, a single auxiliary qubit is introduced. The circuit initializes the system to $|\mathcal{V}\rho_{eq}\rangle$, applies a controlled-Pauli evolution gate for $e^{-i\mathcal{H}_{sch}(\eta)t}$ conditioned on the ancilla being in the $|+\rangle$ state, and measures the ancilla in the X -basis. By iterating this circuit over the discretized Fourier modes η and aggregating the measurement statistics, the generalized non-Hermitian Green's function $\chi(\tau)$ is successfully constructed. The simulation is conducted in a noise-free environment utilizing the Qiskit Sampler primitive, focusing on the discretization errors and the convergence properties of the Schrödingerization approach.

A. Dynamics of Non-Hermitian Response

We calculate the response function $\chi(\tau) = \langle I | (\sigma_x \otimes I) e^{\mathcal{L}\tau} \mathcal{V} | \rho_{eq} \rangle$, where the perturbation \mathcal{V} corresponds to a σ_x drive and the observable is also σ_x . As shown in Fig. 2, we compare the exact analytic Lindblad dynamics (solid black line) against the Sampler-based Schrödingerization simulations evaluated at distinct resolution levels. The low-resolution simulation ($N = 20, L = 5$) captures the qualitative trend but suffers from quantitative deviations due to truncation. As the parameters are increased to a high resolution

($N = 200, L = 40$), the simulated response (blue circles) converges perfectly to the exact Lindblad solution. This multi-resolution overlay definitively demonstrates that the high-dimensional unitary evolution in the extended space meticulously captures the dissipative dynamics of the physical system.

B. Error Convergence and Scaling

The accuracy and efficiency of the continuous-variable Schrödingerization method hinge on two critical numerical parameters: the truncation limit L and the Fourier grid resolution N .

The parameter L defines the finite domain $[-L, L]$ over which the infinite Fourier space integral is truncated. Physically, it dictates how much of the inverse Fourier transform's tail is captured. Because the Fourier transform of the warped state decays slowly as $1/\eta$, L must be chosen sufficiently large to minimize the truncation error and properly reconstruct the exact exponential decaying dynamics.

Conversely, the parameter N defines the number of discrete grid points evaluated within the $[-L, L]$ interval, establishing a grid spacing of $d\eta = L/N$. The time evolution term $e^{-i\eta\mathcal{H}_1 t}$ oscillates with a frequency proportional to the simulation time t . If N is too small for a given L , the spacing $d\eta$ becomes too sparse to resolve these rapid oscillations, leading to severe aliasing (Nyquist sampling error) and resulting in a divergent sum. Therefore, achieving convergence to the exact Lindbladian solution requires monotonically increasing $L \rightarrow \infty$ while simultaneously ensuring that N scales proportionally faster to guarantee $d\eta \rightarrow 0$. In Fig. 3, we analyze the absolute error between the exact and simulated response functions subject to these parameters.

Fig. 3 shows the error convergence with respect to the number of Fourier modes N . Since N is related to the number of auxiliary qubits as $M = \log_2(2N + 1)$, the exponential decay of error indicates that high precision can be achieved with a relatively small number of qubits. Furthermore, Fig. 4 illustrates the dependence on the truncation limit L . The error scales as e^{-L} , which matches the theoretical scaling $\ln(1/\epsilon) \sim L$. These numerical results confirm that the proposed algorithm is not only theoretically robust but also highly efficient for simulating dissipative non-Hermitian systems.

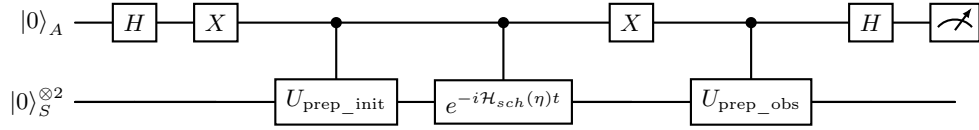


FIG. 1. Quantum circuit for the modified Hadamard test used in the Sampler simulation. The auxiliary qubit A controls the preparation of the initial vectorized state $U_{\text{prep_init}}$ and the Schrödingerization evolution $e^{-i\mathcal{H}_{sch}(\eta)t}$ on the system register S when in the $|0\rangle$ branch. It then controls the preparation of the observable state $U_{\text{prep_obs}}$ on the $|1\rangle$ branch. Measuring the ancilla in the X -basis extracts the real part of the density matrix overlap.

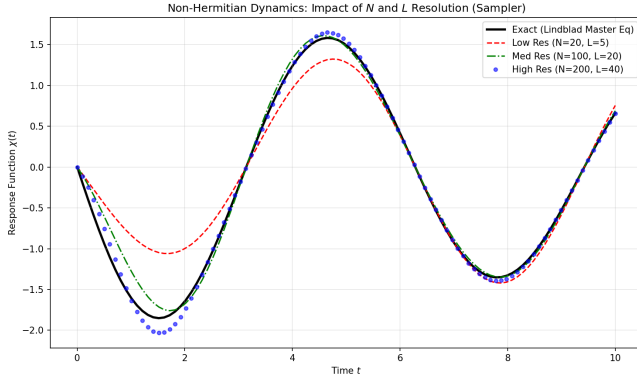


FIG. 2. Numerical simulation of the non-Hermitian linear response function $\chi(\tau)$. The exact solution of the Lindblad master equation (solid black line) is perfectly reproduced by the Schrödingerization simulation (blue circles) with discretized Fourier modes η in the high resolution limit.

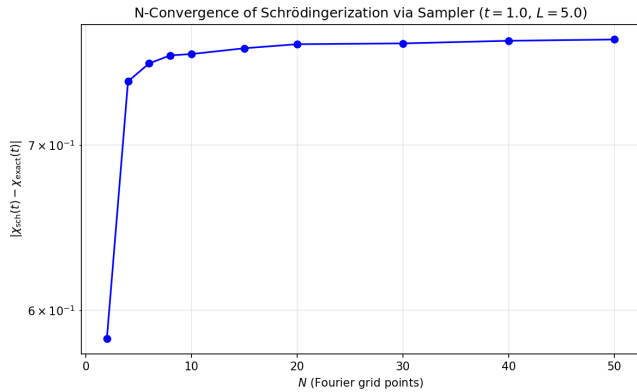


FIG. 3. Error convergence as a function of the number of Fourier grid points N . The log-log plot shows that the precision improves exponentially as N increases, consistent with the theoretical $O(\text{poly}(\log(1/\epsilon)))$ scaling.

V. CONCLUSION

We have demonstrated a structural pathway to evaluating Green's functions and correlation functions of non-Hermitian open quantum systems on quantum computers. By analytically deriving the expanded Hamiltonian for the amplitude damping model, we proved that non-unitary

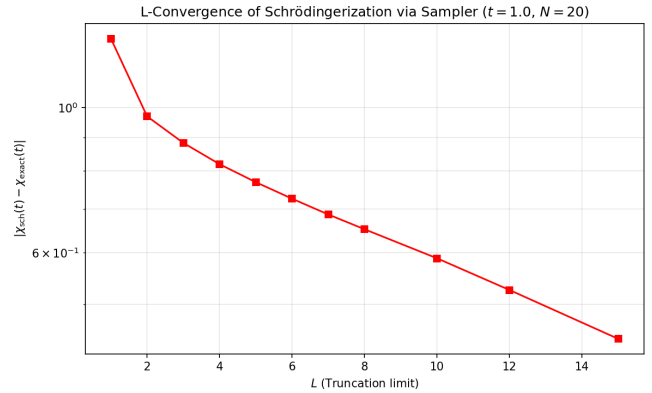


FIG. 4. Impact of the warped variable truncation limit L on the simulation accuracy. The tail error $\epsilon_{\text{tail}} \sim e^{-L}$ decreases exponentially, confirming the theoretical error bound derived in Appendix E.

linear responses can be systematically extracted via the continuous-variable Schrödingerization technique. Bypassing the necessity for complex matrix inversion algorithms and overcoming the non-unitary limitations, this approach broadens the application area of quantum computing in the study of driven-dissipative strongly correlated electron systems and physical chemistry.

Appendix A: Formalism of Vectorization and Liouville Space

The vectorization process, also known as the Choi-Jamiołkowski isomorphism, maps an operator $X \in \mathcal{B}(\mathcal{H})$ in the physical Hilbert space \mathcal{H} to a vector $|X\rangle \in \mathcal{H} \otimes \mathcal{H}^*$ in the Liouville space [6]. For a discrete basis $\{|i\rangle\}$, the mapping is:

$$|i\rangle\langle j| \rightarrow |i\rangle \otimes |j\rangle \equiv |ij\rangle. \quad (\text{A1})$$

The Hilbert-Schmidt inner product in the Liouville space is defined as:

$$\langle A, B \rangle_{HS} = \text{Tr}(A^\dagger B) = \sum_{ij} A_{ij}^* B_{ij}. \quad (\text{A2})$$

The identity operator I becomes a state $|I\rangle = \sum_i |i\rangle \otimes |i\rangle$, such that the expectation value $\text{Tr}(A\rho) = \langle I|(A \otimes I)|\rho\rangle$.

Thus, the Lindblad equation $\dot{\rho} = \mathcal{L}[\rho]$ is recast as a linear ODE $\partial_t |\rho\rangle = \mathcal{L}|\rho\rangle$. More detailed treatments of this formalism can be found in Ref. [5].

Appendix B: Detailed Mechanics of Schrödingerization

The Schrödingerization technique, originally introduced by Jin, Liu, and Yu [4, 10], provides a systematic protocol to map general non-unitary linear differential equations into high-dimensional unitary Schrödinger equations.

Our goal is to simulate the non-Hermitian dynamic equation $\partial_t |\rho\rangle = \mathcal{L}|\rho\rangle$. By decomposing the Liouvillian into its Hermitian and anti-Hermitian components, $\mathcal{L} = \mathcal{H}_1 - i\mathcal{H}_2$ (where $\mathcal{H}_1 = (\mathcal{L} + \mathcal{L}^\dagger)/2$ and $\mathcal{H}_2 = i(\mathcal{L} - \mathcal{L}^\dagger)/2$), we introduce a continuous auxiliary variable $\xi > 0$ and define the warped transformation $w(t, \xi) = e^{-\xi} |\rho(t)\rangle$. This warped state inherently satisfies two simultaneous differential equations:

$$\partial_t w = (\mathcal{H}_1 - i\mathcal{H}_2)w, \quad \text{and} \quad \partial_\xi w = -w. \quad (\text{B1})$$

By substituting the spatial derivative $\partial_\xi w = -w$ into the dynamic equation to eliminate the explicit -1 factor, we couple the real time evolution with the auxiliary dimension:

$$\partial_t w = -\mathcal{H}_1 \partial_\xi w - i\mathcal{H}_2 w. \quad (\text{B2})$$

To diagonalize the differential operator in the augmented dimension, we perform a Fourier transform with respect to ξ , defined as $\tilde{w}(t, \eta) = \int w(t, \xi) e^{-i\eta\xi} d\xi$. Recalling the Fourier identity $\mathcal{F}[\partial_\xi w] = i\eta\tilde{w}$, the equation simplifies into a purely imaginary evolution:

$$i\partial_t \tilde{w}(t, \eta) = (\eta\mathcal{H}_1 + \mathcal{H}_2)\tilde{w}(t, \eta) \equiv \mathcal{H}_{sch}(\eta)\tilde{w}(t, \eta). \quad (\text{B3})$$

Because both \mathcal{H}_1 and \mathcal{H}_2 are Hermitian by construction, the extended effective Hamiltonian $\mathcal{H}_{sch}(\eta)$ is strictly

Hermitian for any real Fourier momentum η . Consequently, the state evolves under a unitary propagator $U(t, \eta) = e^{-i\mathcal{H}_{sch}(\eta)t}$, completely mitigating the spectral instabilities of non-unitary operators.

To recover the physical dynamics of the target open quantum system, one performs the inverse Fourier transform evaluated at the original boundary condition $\xi = 0$:

$$|\rho(t)\rangle = \frac{1}{2\pi} \int_{-\infty}^{\infty} e^{-i\mathcal{H}_{sch}(\eta)t} \tilde{w}(0, \eta) d\eta. \quad (\text{B4})$$

The initial state in momentum space is derived from the ξ -domain initial condition: $\tilde{w}(0, \eta) = \int_0^\infty e^{-\xi} e^{-i\eta\xi} |\rho(0)\rangle d\xi = \frac{1}{1+i\eta} |\rho(0)\rangle$. Thus, the integral evaluates to:

$$|\rho(t)\rangle = \frac{1}{2\pi} \int_{-\infty}^{\infty} \frac{1}{1+i\eta} e^{-i\mathcal{H}_{sch}(\eta)t} |\rho(0)\rangle d\eta. \quad (\text{B5})$$

In practical digital quantum simulation, this integral is numerically evaluated by truncating the bounds to $\eta \in [-L, L]$ and discretizing the momentum space into N grid points, which necessitates mapping the continuous variable into an ancillary multi-qubit register. The resulting simulation workflow scales universally within the framework of standard Hamiltonian simulation paradigms [7].

Appendix C: Derivation of Non-Hermitian Response Functions

Let the total Liouvillian be $\mathcal{L}_{tot}(t) = \mathcal{L} + f(t)\mathcal{V}$. The density matrix evolves as $|\rho(t)\rangle = e^{\mathcal{L}t} |\rho(0)\rangle + \int_0^t dt' e^{\mathcal{L}(t-t')} f(t') \mathcal{V} |\rho(t')\rangle$. In the first-order approximation (weak perturbation), we replace $|\rho(t')\rangle$ with the equilibrium state $|\rho_{eq}\rangle$:

$$\delta |\rho(t)\rangle \approx \int_0^t dt' f(t') e^{\mathcal{L}(t-t')} \mathcal{V} |\rho_{eq}\rangle. \quad (\text{C1})$$

The change in expectation value $\delta \langle A(t) \rangle = \langle I|(A \otimes I)|\delta\rho(t)\rangle$ yields:

$$\delta \langle A(t) \rangle = \int_0^t dt' f(t') \underbrace{\langle I|(A \otimes I)e^{\mathcal{L}(t-t')} \mathcal{V} |\rho_{eq}\rangle}_{\chi(t-t')}. \quad (\text{C2})$$

This derivation mirrors the Kubo formalism but allows for non-Hermitian generators \mathcal{L} that include dissipation.

Appendix D: Performance Under Realistic Hardware Noise

The transformation requires continuous-variable quantum modes or highly discretized qubit registers. A primary challenge in implementing the inverse quantum Fourier transform (IQFT) [13] on near-term devices is

its sensitivity to depolarizing noise, largely due to the high circuit depth and the large number of multi-qubit controlled gates required as the precision increases. For discretized registers, these gates accumulate errors that can significantly degrade the fidelity of the final state reconstruction. We leave the rigorous resource estimation and specific error mitigation strategies to future work.

Appendix E: Derivation of Complexity Scaling for Schrödingerization

The precision ϵ of the Schrödingerization approach depends on two primary factors: the truncation of the warped variable ξ and the discretization of the Fourier space η .

Consider the transformation $w(t, \xi) = e^{-\xi} |\rho(t)\rangle$. To ensure that the state remains within a finite domain $\xi \in [0, L]$, we must choose L such that the tail e^{-L} is

negligible. For a target precision ϵ , we require $e^{-L} \leq \epsilon$, which implies $L \geq \ln(1/\epsilon)$.

The Fourier modes η are discretized as $\eta_j = j\Delta\eta$ for $j = -N, \dots, N$. The number of qubits required for the auxiliary register is $M = \log_2(2N + 1)$. According to the error analysis in Ref. [10], the total error ϵ scales with the mesh size $\Delta\xi$ and the spectral range of \mathcal{L} . Crucially, the gate complexity for evolving the unitary Schrödingerized Hamiltonian $\mathcal{H}_{sch}(\eta)$ using a k -th order Trotter-Suzuki decomposition scales as $O(t \cdot \text{poly}(\log(1/\epsilon)))$, which is an exponential improvement over the $O(1/\epsilon)$ scaling seen in traditional first-generation dilated solvers.

Furthermore, unlike QSVT [12] which requires building a block-encoding for a non-unitary \mathcal{L} , Schrödingerization only requires the capability to simulate the Hermitian parts \mathcal{H}_1 and \mathcal{H}_2 . This bypasses the often-expensive subroutines for preparing the oracle for $A^\dagger A$ or specific singular value transformations, leading to the optimal state preparation cost discussed in Section II.

-
- [1] R. Kubo, The fluctuation-dissipation theorem, [Reports on Progress in Physics](#) **29**, 255 (1966).
 - [2] D. Manzano, A short introduction to the lindblad master equation, [AIP Advances](#) **10**, 025106 (2020).
 - [3] L. Pan, X. Chen, Y. Chen, and H. Zhai, Non-hermitian linear response theory, [Nature Physics](#) **16**, 767–771 (2020).
 - [4] S. Jin, N. Liu, and Y. Yu, Quantum simulation of partial differential equations via schrödingerization, [Phys. Rev. Lett.](#) **133**, 230602 (2024).
 - [5] J. A. Gyamfi, Fundamentals of quantum mechanics in liouville space, [European Journal of Physics](#) **41**, 063002 (2020).
 - [6] H.-P. Breuer and F. Petruccione, *The Theory of Open Quantum Systems* (Oxford University Press, 2002).
 - [7] J. Hu, S. Jin, N. Liu, and L. Zhang, Quantum Circuits for partial differential equations via Schrödingerisation, [Quantum](#) **8**, 1563 (2024).
 - [8] D. Motlagh and N. Wiebe, Generalized quantum signal processing, [PRX Quantum](#) **5**, 020368 (2024).
 - [9] D. An, J.-P. Liu, and L. Lin, Linear combination of hamiltonian simulation for nonunitary dynamics with optimal state preparation cost, [Phys. Rev. Lett.](#) **131**, 150603 (2023).
 - [10] S. Jin, N. Liu, and C. Ma, Schrödingerization based computationally stable algorithms for ill-posed problems in partial differential equations, [SIAM Journal on Numerical Analysis](#) (2024).
 - [11] A. W. Harrow, A. Hassidim, and S. Lloyd, Quantum algorithm for solving linear systems of equations, [Phys. Rev. Lett.](#) **103**, 150502 (2009).
 - [12] A. Gilyén, Y. Su, G. H. Low, and N. Wiebe, Quantum singular value transformation and beyond: exponential speedups for matrix functions, quantum schor amplitude amplification and polynomial approximations, in [Proceedings of the 51st Annual ACM SIGACT Symposium on Theory of Computing](#) (2019) pp. 193–204.
 - [13] M. A. Nielsen and I. L. Chuang, *Quantum Computation and Quantum Information*, 10th ed. (Cambridge University Press, 2010).